Pergamon

Int. J. Solids Structures Vol. 34, No. 26, pp. 3401–3414, 1997

0020–7683/97 $17.00 + .00

PII: S0020–7683(96)00221–1

ELECTROELASTIC ANALYSIS OF A PIEZOELECTRIC ELLIPTICAL INHOMOGENEITY

S. A. MEGUID and Z. ZHONG†
Engineering Mechanics and Design Laboratory, Department of Mechanical and Industrial Engineering, University of Toronto, 5 King's College Road, Toronto, Canada M5S 3G8

(*Received* 20 *March* 1996; *in revised form* 2 *August* 1996)

Abstract—This paper is concerned with the development of a general solution for the elliptical inhomogeneity problem in piezoelectric materials under antiplane shear and inplane electric field. *Explicit* forms of the electroelastic fields are given in both the inhomogeneity and the matrix by means of the complex variable method. Furthermore, the change of the electric enthalpy due to the presence of an inhomogeneity is obtained. Numerical examples are provided to show the effect of the material mismatch, the aspect ratio of the inhomogeneity and the loading condition upon the change of the electric enthalpy and the electroelastic field concentration due to the presence of the inhomogeneity. © 1997 Elsevier Science Ltd.

1. INTRODUCTION

In view of their intrinsic electro-mechanical coupling characteristics and the potential for use in applications involving smart and adaptive material systems, piezoelectric ceramics are receiving increased attention from the scientific community. Electroelastic field concentrations at defects or inhomogeneities such as cracks, voids or particles in a piezoelectric composite material can contribute to critical crack growth and subsequent mechanical failure or dielectric breakdown. Therefore, it is of vital importance to study the electroelastic fields as a result of the presence of defects or inhomogeneities in these quasi-brittle solids.

Numerous attempts have been made to analyze a crack or a dislocation in piezoelectric materials, see for example the works of Barnett and Lothe (1975), McMeeking (1989), Pak (1990), Sosa and Pak (1990), Suo *et al.* (1992), Yang and Suo (1994), among others. Attempts have also been made to treat the inhomogeneity problem in this class of materials. Typical examples include the work of Deeg (1980) and Dunn and Taya (1993) who extended the application of the equivalent inclusion method of Eshelby (1957) to piezoelectric materials. More recently, Pak (1992) studied the antiplane problem of a piezoelectric circular inclusion, while Dunn (1994a) obtained the electroelastic field around an elliptical void or a flaw in a piezoelectric solid. Furthermore, Dunn (1994b) obtained the electroelastic Green's functions for transversely isotropic piezoelectric media. Liang *et al.* (1995) obtained the coupled electroelastic field inside the inhomogeneity and on the interface. In addition, Schulgasser (1992) and Chen (1993) established exact relations between the effective properties of piezoelectric composites. However, only a limited number of attempts have been made to explicitly determine the electroelastic field in the matrix, which is the subject of the current study.

In the present paper, we provide a general solution for the elliptical inhomogeneity problem in piezoelectric materials under antiplane shear and inplane electric field. Firstly, *explicit* forms of the electroelastic fields are given in both the inhomogeneity and the matrix by means of the complex variable method. Furthermore, the change of the electric enthalpy due to the presence of an inhomogeneity is obtained. Numerical examples are provided to examine the effect of the material mismatch, the aspect ratio of the inhomogeneity and the

† On sabbatical leave from the Department of Engineering Mechanics and Industrial Technology, Tongji University, Shanghai 200092, P.R. China.

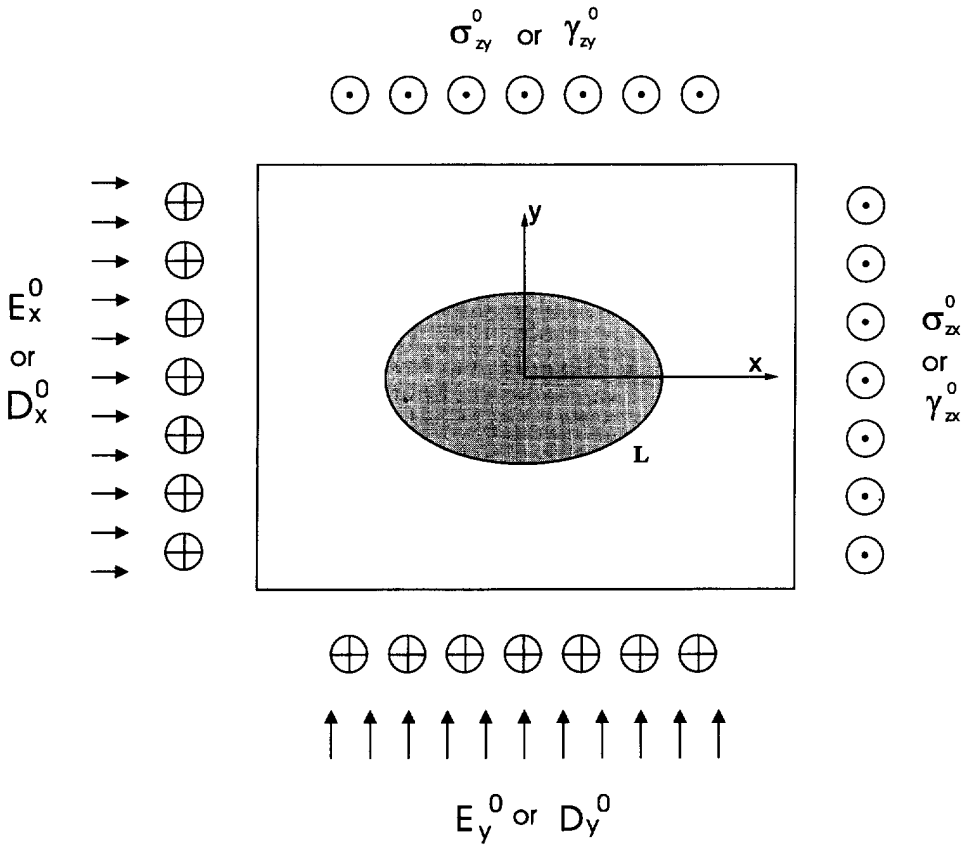

Fig. 1. A schematic of the elliptical piezoelectric inhomogeneity problem under consideration.

loading condition upon the change of the electric enthalpy and the electroelastic field concentration due to the presence of the inhomogeneity.

2. PROBLEM FORMULATION

Consider an elliptical piezoelectric inhomogeneity embedded in an unbounded piezoelectric matrix. The elliptical inhomogeneity, whose major and minor diameters are denoted by $2a$ and $2b$ (focal length $c=(a^2-b^2)^{1/2}$) is oriented with its major and minor axes along the x and y axes, respectively. The inhomogeneity and the matrix have different elastic and electric properties and are assumed to be transversely isotropic with respect to the longitudinal direction. The matrix is subjected to a remote inplane (x–y plane) electric fields as well as out of plane shear, as shown in Fig. 1. The inhomogeneity is assumed to be perfectly bonded with the matrix at the interface L. The regions occupied by the matrix and the inhomogeneity will be referred to as regions 1 and 2, respectively. In addition, the quantities associated with the matrix and the inhomogeneity will be denoted by the corresponding superscripts or subscripts.

For this problem, the out-of-plane displacement w and the electric potential ϕ are only functions of the variables x and y, such that $w = w(x, y)$ and $\phi = \phi(x, y)$.

For linear piezoelectric materials, the electric enthalpy density can be expressed as (Pak, 1990)

$$h=\tfrac{1}{2}G_L(\gamma_{zx}^2+\gamma_{zy}^2)-\tfrac{1}{2}k_{11}(E_x^2+E_y^2)-e_{15}(\gamma_{zx}E_x+\gamma_{zy}E_y) \tag{1}$$

where γ_{zx} and γ_{zy} are the shear strains, E_x and E_y are the electric fields, G_L is the longitudinal shear modulus, e_{15} denotes the piezoelectric modulus and k_{11} represents the dielectric

modulus. The first term of eqn (1) is the energy stored in the deformation, the second term is the energy stored in the electric fields and the last terms is the interaction energy.

The equilibrium equations for the stresses and the electric displacements are

$$\frac{\partial \sigma_{zx}}{\partial x}+\frac{\partial \sigma_{zy}}{\partial y}=0$$
$$\frac{\partial D_x}{\partial x}+\frac{\partial D_y}{\partial y}=0 \tag{2}$$

where σ_{zx} and σ_{zy} are the shear stresses, while D_x and D_y are the electric displacements.

The constitutive relations can be written as

$$\sigma_{zx}=\frac{\partial h}{\partial \gamma_{zx}}=G_L\gamma_{zx}-e_{15}E_x$$
$$\sigma_{zy}=\frac{\partial h}{\partial \gamma_{zy}}=G_L\gamma_{zy}-e_{15}E_y$$
$$D_x=-\frac{\partial h}{\partial E_x}=e_{15}\gamma_{zx}+k_{11}E_x$$
$$D_y=-\frac{\partial h}{\partial E_y}=e_{15}\gamma_{zy}+k_{11}E_y. \tag{3}$$

The shear strains γ_{zx} and γ_{zy} and the electric fields E_x and E_y are related to the displacement w and the electric potential ϕ by the following form:

$$\gamma_{zx}=\frac{\partial w}{\partial x}\quad \gamma_{zy}=\frac{\partial w}{\partial y}\quad E_x=-\frac{\partial \phi}{\partial x}\quad E_y=-\frac{\partial \phi}{\partial y}. \tag{4}$$

Substituting (3) and (4) into (2), we obtain the governing equations:

$$\nabla^2 w=0\quad \nabla^2\phi=0 \tag{5}$$

where ∇^2 is the Laplacian operator.

Equation (5) indicates that w and ϕ are harmonic functions which can be taken as the real part of some analytic functions of the complex variable $z=x+iy$, such that

$$w=\frac{1}{2G_L}(\Psi(z)+\overline{\Psi(z)})$$
$$\phi=\frac{1}{2k_{11}}(\Phi(z)+\overline{\Phi(z)}) \tag{6}$$

where Ψ and Φ represent the analytic functions and the overbar denotes the complex conjugate. Hence, the stresses and the electric displacements can be expressed as

$$\sigma_{zx}-i\sigma_{zy}=\Psi'(z)+\frac{e_{15}}{k_{11}}\Phi'(z)$$
$$D_x-iD_y=\frac{e_{15}}{G_L}\Psi'(z)-\Phi'(z) \tag{7}$$

where the prime denotes the derivative with respect to the argument.

In order to define the continuity conditions at the inhomogeneity-matrix interface, we introduce two quantities:

$$T = \int_A^B (\sigma_{zx}\,dy - \sigma_{zy}\,dx)$$

$$= \frac{i}{2}\left\{[\overline{\Psi(z)} - \Psi(z)]_A^B + \frac{e_{15}}{k_{11}}[\overline{\Phi(z)} - \Phi(z)]_A^B\right\}$$

$$S = \int_A^B (D_x\,dy - D_y\,dx)$$

$$= \frac{i}{2}\left\{\frac{e_{15}}{G_L}[\overline{\Psi(z)} - \Psi(z)]_A^B - [\overline{\Phi(z)} - \Phi(z)]_A^B\right\} \tag{8}$$

where T is the resultant force along any arc AB and S is the sum of the normal component of the electric displacement along arc AB; $[\ ]_A^B$ denotes the change in the bracketed function in going from A to point B along the arc.

The assumption of perfect bonding between regions 1 and 2 implies that

$$w_1 = w_2 \quad \phi_1 = \phi_2 \quad T_1 = T_2 \quad B_1 = B_2 \quad \text{on } L. \tag{9}$$

3. SOLUTION

Using the approach of conformal transformation (see, e.g., Gong and Meguid, 1992, 1993), it can be shown that the complex potentials, which satisfy the governing eqn (5) and the boundary condition (9), have the following form:

$$\Psi_1(z) = (P_0^\bullet + iP_0^*)z + (K_0^\bullet + iK_0^*)[z - (z^2 - c^2)^{1/2}] \tag{10}$$

$$\Phi_1(z) = (Q_0^\bullet + iQ_0^*)z + (M_0^\bullet + iM_0^*)[z - (z^2 - c^2)^{1/2}] \tag{11}$$

in the matrix, and

$$\Psi_2(z) = (G_0^\bullet + iG_0^*)z \tag{12}$$

$$\Phi_2(z) = (H_0^\bullet + iH_0^*)z \tag{13}$$

in the inhomogeneity, where

$$\begin{Bmatrix} G_0^\bullet \\ G_0^* \end{Bmatrix} = (I_0^{(1)} \pm J_0^{(1)}) \begin{Bmatrix} P_0^\bullet \\ P_0^* \end{Bmatrix} + (L_0^{(1)} \pm N_0^{(1)}) \begin{Bmatrix} Q_0^\bullet \\ Q_0^* \end{Bmatrix} \tag{14}$$

$$\begin{Bmatrix} H_0^\bullet \\ H_0^* \end{Bmatrix} = (I_0^{(3)} \pm J_0^{(3)}) \begin{Bmatrix} P_0^\bullet \\ P_0^* \end{Bmatrix} + (L_0^{(3)} \pm N_0^{(3)}) \begin{Bmatrix} Q_0^\bullet \\ Q_0^* \end{Bmatrix} \tag{15}$$

$$\begin{Bmatrix} K_0^\bullet \\ K_0^* \end{Bmatrix} = \frac{1}{2}\left\{[(I_0^{(2)} \pm J_0^{(2)})R^2 - 1] \begin{Bmatrix} P_0^\bullet \\ P_0^* \end{Bmatrix} + (L_0^{(2)} \pm N_0^{(2)})R^2 \begin{Bmatrix} Q_0^\bullet \\ Q_0^* \end{Bmatrix}\right\} \tag{16}$$

$$\begin{Bmatrix} M_0^\bullet \\ M_0^* \end{Bmatrix} = \frac{1}{2}\left\{(I_0^{(4)} \pm J_0^{(4)})R^2 \begin{Bmatrix} P_0^\bullet \\ P_0^* \end{Bmatrix} + [(L_0^{(4)} \pm N_0^{(4)})R^2 - 1] \begin{Bmatrix} Q_0^\bullet \\ Q_0^* \end{Bmatrix}\right\} \tag{17}$$

with

$$R=\left(\frac{a+b}{a-b}\right)^{1/2} \tag{18}$$

and $I_0^{(n)}$, $J_0^{(n)}$, $L_0^{(n)}$ and $N_0^{(n)}$ $(n=1,4)$ are given in the Appendix. In these equations, $P_0^{\bullet}$, P_0^{*}, $Q_0^{\bullet}$ and Q_0^{*} are real quantities, which will be determined from the far-field loading conditions. Substituting (10)–(13) into (6) and (7), we obtain the electroelastic fields, as follows:

$$w_1=\frac{r}{G_L^1}\left[(P_0^{\bullet}+K_0^{\bullet})\cos\theta-(P_0^{*}+K_0^{*})\sin\theta - \frac{\sqrt{r_1r_2}}{r}K_0^{\bullet}\cos\left(\frac{\theta_1+\theta_2}{2}\right)+\frac{\sqrt{r_1r_2}}{r}K_0^{*}\sin\left(\frac{\theta_1+\theta_2}{2}\right)\right] \tag{19}$$

$$\phi_1=\frac{r}{k_{11}^1}\left[(Q_0^{\bullet}+M_0^{\bullet})\cos\theta-(Q_0^{*}+M_0^{*})\sin\theta - \frac{\sqrt{r_1r_2}}{r}M_0^{\bullet}\cos\left(\frac{\theta_1+\theta_2}{2}\right)+\frac{\sqrt{r_1r_2}}{r}M_0^{*}\sin\left(\frac{\theta_1+\theta_2}{2}\right)\right] \tag{20}$$

$$\sigma_{zx1}=P_0^{\bullet}+K_0^{\bullet}+\frac{e_{15}^1}{k_{11}^1}(Q_0^{\bullet}+M_0^{\bullet})-\left(K_0^{\bullet}+\frac{e_{15}^1}{k_{11}^1}M_0^{\bullet}\right)\frac{r}{\sqrt{r_1r_2}}\cos\left(\theta-\frac{\theta_1+\theta_2}{2}\right) +\left(K_0^{*}+\frac{e_{15}^1}{k_{11}^1}M_0^{*}\right)\frac{r}{\sqrt{r_1r_2}}\sin\left(\theta-\frac{\theta_1+\theta_2}{2}\right) \tag{21}$$

$$\sigma_{zy1}=-(P_0^{*}+K_0^{*})-\frac{e_{15}^1}{k_{11}^1}(Q_0^{*}+M_0^{*})+\left(K_0^{\bullet}+\frac{e_{15}^1}{k_{11}^1}M_0^{\bullet}\right)\frac{r}{\sqrt{r_1r_2}}\sin\left(\theta-\frac{\theta_1+\theta_2}{2}\right) +\left(K_0^{*}+\frac{e_{15}^1}{k_{11}^1}M_0^{*}\right)\frac{r}{\sqrt{r_1r_2}}\cos\left(\theta-\frac{\theta_1+\theta_2}{2}\right) \tag{22}$$

$$D_{x1}=\frac{e_{15}^1}{G_L^1}(P_0^{\bullet}+K_0^{\bullet})-(Q_0^{\bullet}+M_0^{\bullet})-\left(\frac{e_{15}^1}{G_L^1}K_0^{\bullet}-M_0^{\bullet}\right)\frac{r}{\sqrt{r_1r_2}}\cos\left(\theta-\frac{\theta_1+\theta_2}{2}\right) +\left(\frac{e_{15}^1}{G_L^1}K_0^{*}-M_0^{*}\right)\frac{r}{\sqrt{r_1r_2}}\sin\left(\theta-\frac{\theta_1+\theta_2}{2}\right) \tag{23}$$

$$D_{y1}=-\frac{e_{15}^1}{G_L^1}(P_0^{*}+K_0^{*})+(Q_0^{*}+M_0^{*})+\left(\frac{e_{15}^1}{G_L^1}K_0^{\bullet}-M_0^{\bullet}\right)\frac{r}{\sqrt{r_1r_2}}\sin\left(\theta-\frac{\theta_1+\theta_2}{2}\right) +\left(\frac{e_{15}^1}{G_L^1}K_0^{*}-M_0^{*}\right)\frac{r}{\sqrt{r_1r_2}}\cos\left(\theta-\frac{\theta_1+\theta_2}{2}\right) \tag{24}$$

the matrix, and

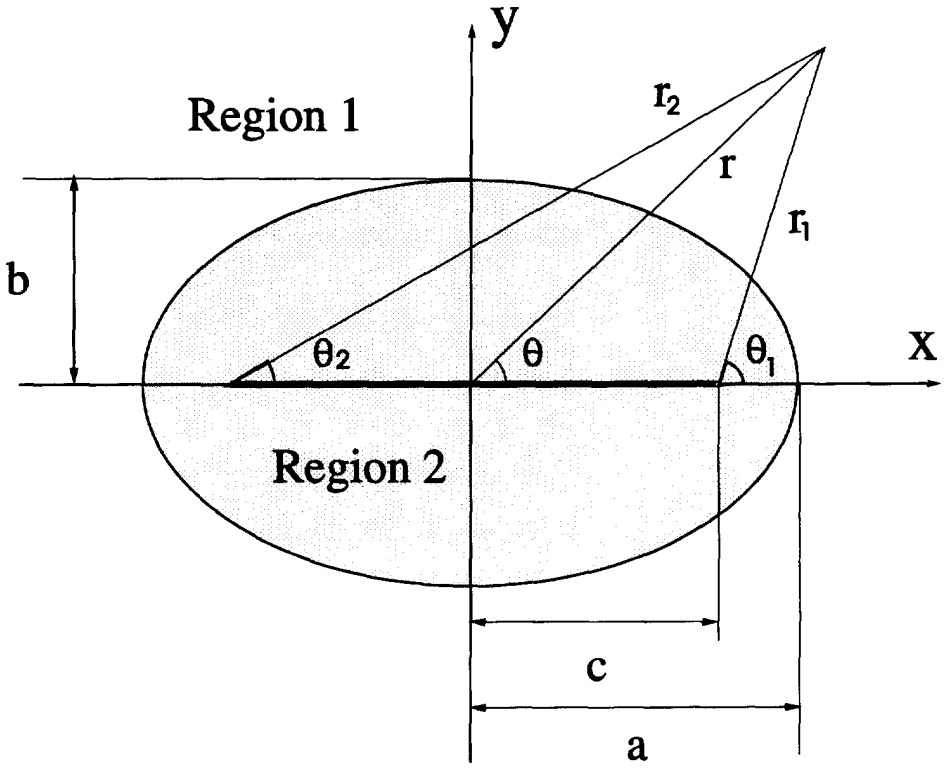

Fig. 2. A schematic of the coordinate used.

$$w_2 = \frac{r}{G_L^2}(G_0^{\bullet}\cos\theta - G_0^{*}\sin\theta) \tag{25}$$

$$\phi_2 = \frac{r}{k_{11}^2}(H_0^{\bullet}\cos\theta - H_0^{*}\sin\theta) \tag{26}$$

$$\sigma_{zx2} = G_0^{\bullet} + \frac{e_{15}^2}{k_{11}^2}H_0^{\bullet} \tag{27}$$

$$\sigma_{zy2} = -G_0^{*} - \frac{e_{15}^2}{k_{11}^2}H_0^{*} \tag{28}$$

$$D_{x2} = \frac{e_{15}^2}{G_L^2}G_0^{\bullet} - H_0^{\bullet} \tag{29}$$

$$D_{y2} = -\frac{e_{15}^2}{G_L^2}G_0^{*} + H_0^{*} \tag{30}$$

in the inhomogeneity, where r and θ are defined in Fig. 2. By applying the far-field loading conditions (Pak, 1990), $P_0^{\bullet}$, P_0^{*}, $Q_0^{\bullet}$ and Q_0^{*} are evaluated as follows:

Case 1: the matrix is subjected to uniform strains γ_{zx}^0 and γ_{zy}^0 as well as uniform electric fields E_x^0 and E_y^0 at infinity. In this case, we have

$$P_0^{\bullet} = G_L^1\gamma_{zx}^0 \tag{31}$$

$$P_0^{*} = -G_L^1\gamma_{zy}^0 \tag{32}$$

$$Q_0^{\bullet} = -k_{11}^1 E_x^0 \tag{33}$$

$$Q_0^* = k_{11}^1 E_y^0. \tag{34}$$

Case 2: the matrix is subjected to uniform stresses σ_{zx}^0 and σ_{zy}^0 as well as uniform electric displacements D_x^0 and D_y^0 at infinity. In this case, we can determine

$$P_0^{\bullet} = \frac{G_L^1(k_{11}^1\sigma_{zx}^0 + e_{15}^1 D_x^0)}{G_L^1 k_{11}^1 + (e_{15}^1)^2} \tag{35}$$

$$P_0^* = -\frac{G_L^1(k_{11}^1\sigma_{zy}^0 + e_{15}^1 D_y^0)}{G_L^1 k_{11}^1 + (e_{15}^1)^2} \tag{36}$$

$$Q_0^{\bullet} = \frac{k_{11}^1(e_{15}^1\sigma_{zx}^0 - G_L^1 D_x^0)}{G_L^1 k_{11}^1 + (e_{15}^1)^2} \tag{37}$$

$$Q_0^* = -\frac{k_{11}^1(e_{15}^1\sigma_{zy}^0 - G_L^1 D_y^0)}{G_L^1 k_{11}^1 + (e_{15}^1)^2}. \tag{38}$$

Case 3: the matrix is subjected to uniform strains γ_{zx}^0 and γ_{zy}^0 as well as uniform electric displacements D_x^0 and D_y^0 at infinity. In this case, we obtain

$$P_0^{\bullet} = G_L^1\gamma_{zx}^0 \tag{39}$$

$$P_0^* = -G_L^1\gamma_{zy}^0 \tag{40}$$

$$Q_0^{\bullet} = e_{15}^1\gamma_{zx}^0 - D_x^0 \tag{41}$$

$$Q_0^* = -e_{15}^1\gamma_{zy}^0 + D_y^0. \tag{42}$$

Case 4: the matrix is subjected to uniform stresses σ_{zx}^0 and σ_{zy}^0 as well as uniform electric fields D_x^0 and D_y^0 at infinity. In this case, we can find

$$P_0^{\bullet} = \sigma_{zx}^0 + e_{15}^1 E_x^0 \tag{43}$$

$$P_0^* = -\sigma_{zy}^0 - e_{15}^1 E_y^0 \tag{44}$$

$$Q_0^{\bullet} = -k_{11}^1 E_x^0 \tag{45}$$

$$Q_0^* = k_{11}^1 E_y^0. \tag{46}$$

It can be observed from (27)–(30) that the stress and electric fields are constant within the elliptical inhomogeneity which confirms the results of Wang (1992), Benveniste (1992) and Dunn (1994). The main contribution of the present solution is in its ability to determine the electroelastic field in the matrix explicitly. In fact, our solution reduces to the earlier results of Pak for the special case of a circular inhomogeneity (Pak, 1992) and an elliptical void (Pak, 1990).

Another interesting aspect of the present solution is the ability to determine the change of the total electric enthalpy in the body due to the introduction of an inhomogeneity. The total electric enthalpy H in a piezoelectric solid of unit thickness and cross-sectional area D can be written as

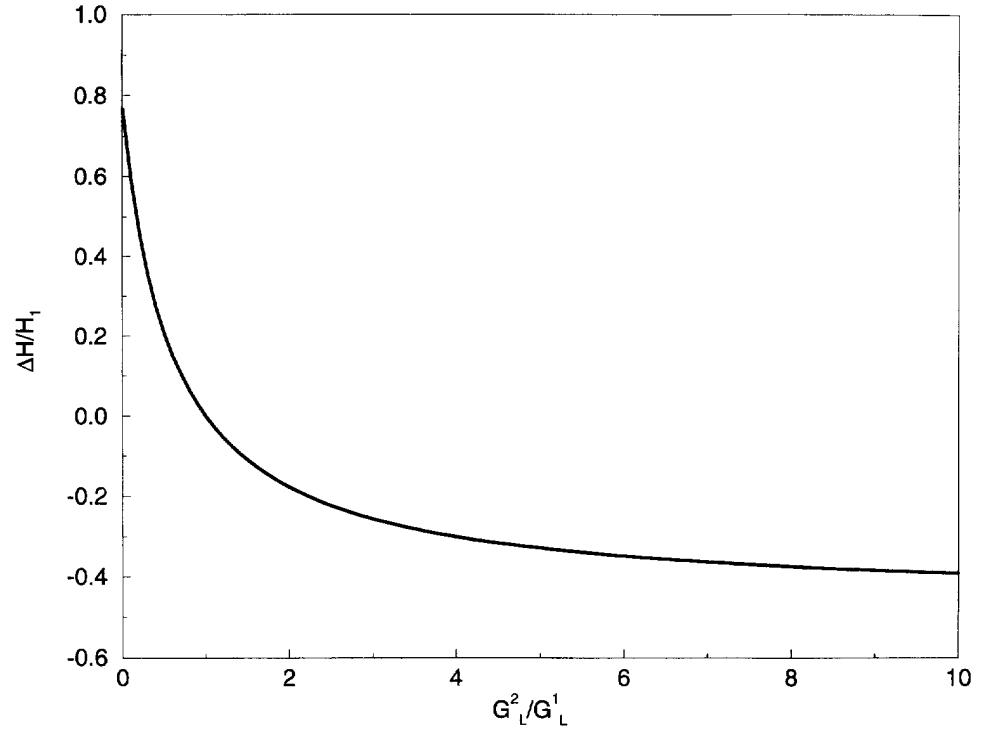

Fig. 3. Variations of the normalized electric enthalpy $\Delta H/H_1$ vs the shear moduli ratio G_L^2/G_L^1.

$$H = \int\int_D h \, \mathrm{d}s \tag{47}$$

where h is the electric enthalpy density given by (1). It can be shown that

$$H = H_0 + \Delta H \tag{48}$$

where H_0 is the electric enthalpy in the absence of inhomogeneities and ΔH represents the contribution due to the introduction of an inhomogeneity. Following the approach used by Gong and Meguid (1992, 1993), ΔH can be evaluated as

$$\Delta H = \frac{\pi c^2}{2}\left[\frac{1}{G_L^1}(P_0^{\bullet}K_0^{\bullet} - P_0^{*}K_0^{*}) - \frac{1}{k_{11}^1}(Q_0^{\bullet}M_0^{\bullet} - Q_0^{*}M_0^{*}) + \frac{e_{15}^1}{G_L^1 k_{11}^1}(P_0^{\bullet}M_0^{\bullet} + Q_0^{\bullet}K_0^{\bullet} - P_0^{*}M_0^{*} - Q_0^{*}K_0^{*})\right]. \tag{49}$$

4. NUMERICAL RESULTS AND DISCUSSION

In this section, we examine the effect of the material mismatch between the inhomogeneity and the matrix, the aspect ratio of the inhomogeneity and the loading condition upon the change of the electric enthalpy and the electroelastic field concentrations due to the presence of the inhomogeneity.

As an example, let us consider an elliptical inhomogeneity with an aspect ratio $a/b = 3$, embedded in an infinite matrix subjected to remote uniform stress and electric field, such that: $\sigma_{zy}^0 = 5 \times 10^7$ N/m^2, $\sigma_{zx}^0 = 0$, $E_y^0 = 10^6$ V/m and $E_x^0 = 0$.

Figure 3 shows the variation of the normalized electric enthalpy $\Delta H/H_1$ vs shear moduli ratio G_L^2/G_L^1. The inhomogeneity and the matrix are assumed to have the same dielectric and piezoelectric moduli: $k_{11}^1 = k_{11}^2 = 1.51 \times 10^{-8}$ C/Vm, $e_{15}^1 = e_{15}^2 = 10.0$ C/m^2 and

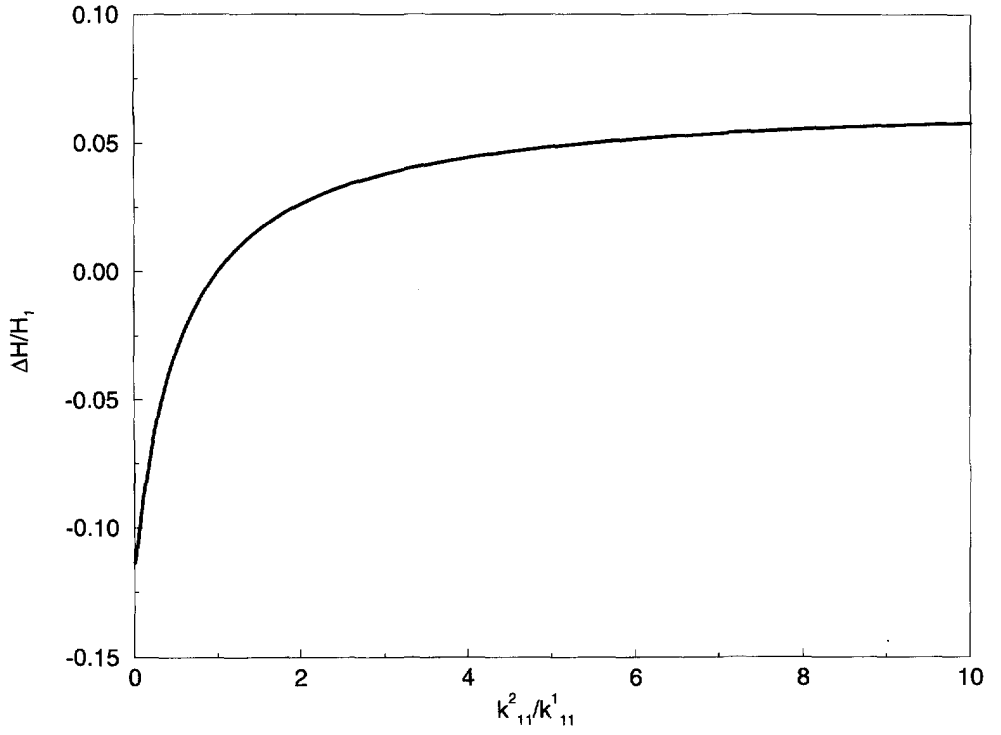

Fig. 4. Variations of the normalized electric enthalpy $\Delta H/H_1$ vs the dielectric moduli ratio k_{11}^2/k_{11}^1.

$G_L^1 = 3.53 \times 10^{10}$ N/m^2. H_1 is an energy factor used to normalize the electric enthalpy and is given by:

$$H_1 = \frac{\pi a^2}{G_L^1}[(P_0^{\bullet})^2 + (P_0^*)^2] + \frac{\pi a^2}{k_{11}^1}[(Q_0^{\bullet})^2 + (Q_0^*)^2]. \tag{50}$$

It is observed from Fig. 3 that an increase in G_L^2/G_L^1 results in a sharp decline in ΔH when the inhomogeneity is softer than the matrix ($G_L^2/G_L^1 < 1$). In the case where the inhomogeneity is harder ($G_L^2/G_L^1 > 1$), the decline is rather gradual approaching asymptotically the case of a rigid inhomogeneity. The figure also reveals that for $G_L^2/G_L^1 \geqslant 5$, the elastic inhomogeneity can be treated as a rigid body.

Figure 4 shows the variation of the normalized electric enthalpy $\Delta H/H_1$ vs the dielectric moduli ratio k_{11}^2/k_{11}^1. The inhomogeneity and the matrix are assumed to have the same shear and piezoelectric moduli: $G_L^1 = 3.53 \times 10^{10}$ N/m^2, $e_{15}^1 = e_{15}^2 = 10.0$ C/m^2 and $k_{11}^1 = 1.51 \times 10^{-8}$ C/Vm. It is observed that with the increase of k_{11}^2/k_{11}^1, ΔH increases sharply when the dielectric modulus of the inhomogeneity is less than that of the matrix, but increases gradually approaching asymptotically the case of a conducting inhomogeneity when the dielectric modulus of the inhomogeneity is greater than that of the matrix. The figure also reveals that for $k_{11}^2/k_{11}^1 \geqslant 5$, the dielectric inhomogeneity can be treated as a conductor.

Figure 5 shows the variation of the normalized electric enthalpy $\Delta H/H_1$ vs the piezoelectric moduli ratio e_{15}^2/e_{15}^1. The inhomogeneity and the matrix are assumed to have the same shear and dielectric moduli: $G_L^1 = G_L^2 = 3.53 \times 10^{10}$ N/m^2, $k_{11}^1 = k_{11}^2 = 1.51 \times 10^{-8}$ C/Vm and $e_{15}^1 = 10.0$ C/m^2. It can be observed from this figure that $\Delta H/H_1$ experiences a sudden jump from -0.46 at $e_{15}^2/e_{15}^1 = -3.0$ to 0.08 at $e_{15}^2/e_{15}^1 = 3.0$. This jump is caused by the mismatch of the piezoelectric moduli between the inhomogeneity and the matrix.

Figure 6 shows the variation of the normalized electric enthalpy $\Delta H/H_1$ vs the aspect ratio of the elliptical inhomogeneity for different ratios of shear moduli. The inhomogeneity and the matrix have the following material constants: $G_L^1 = 3.53 \times 10^{10}$ N/m^2, $k_{11}^1 = k_{11}^2 = 1.51 \times 10^{-8}$ C/Vm, $e_{15}^1 = 10.0$ C/m^2 and $e_{15}^2 = 0$. It can be observed that ΔH

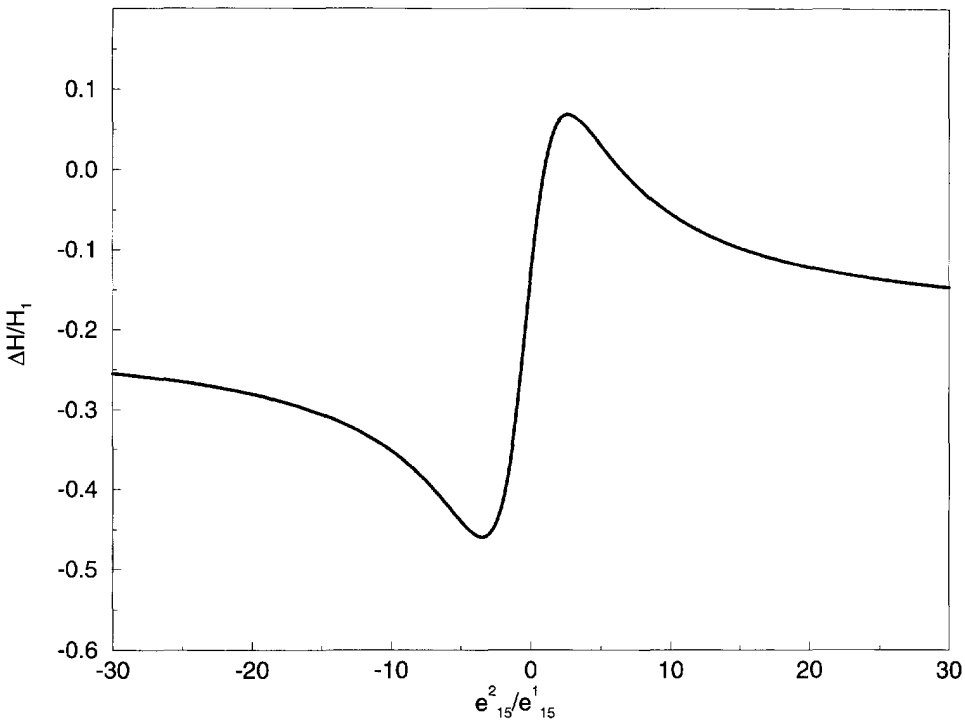

Fig. 5. Variations of the normalized electric enthalpy $\Delta H/H_1$ vs the piezoelectric moduli ratio e_{15}^2/e_{15}^1.

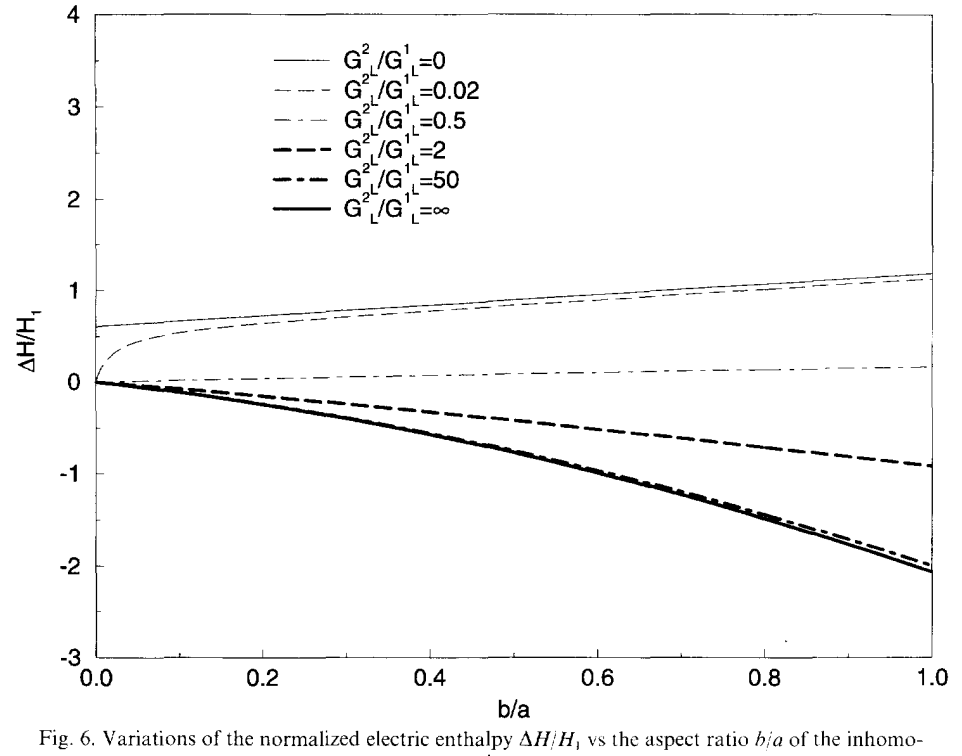

Fig. 6. Variations of the normalized electric enthalpy $\Delta H/H_1$ vs the aspect ratio b/a of the inhomogeneity.

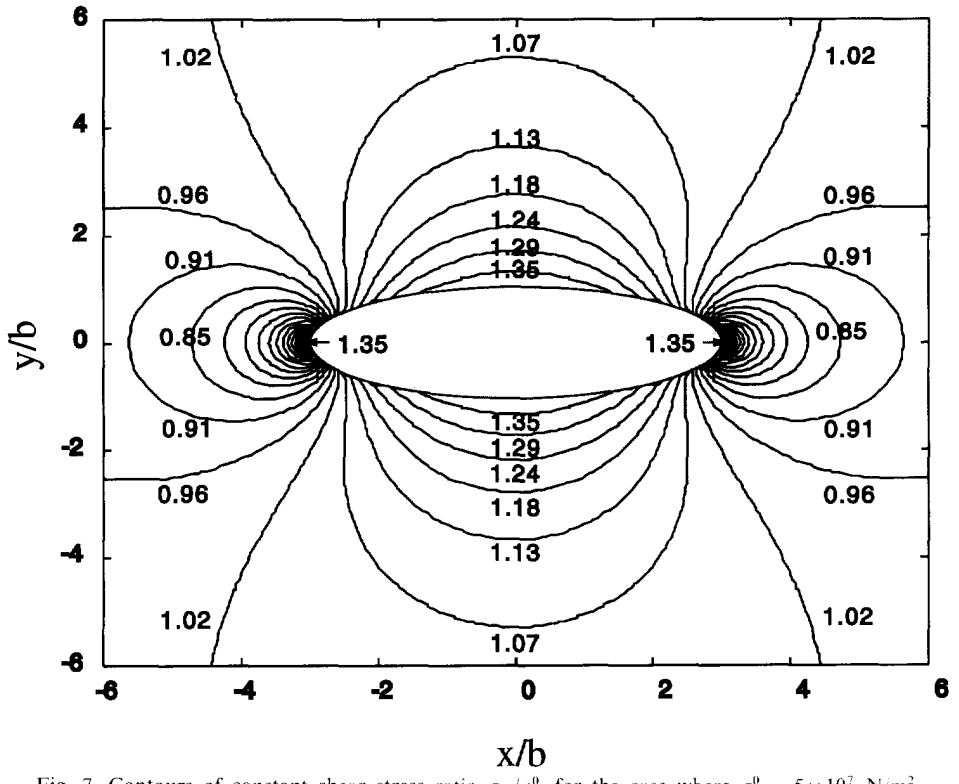

Fig. 7. Contours of constant shear stress ratio $\sigma_{zy}/\sigma^0_{zy}$ for the case where $\sigma^0_{zy} = 5\times10^7$ N/m^2, $\sigma^0_{zx} = 0$, $E^0_y = 10^6$ V/m and $E^0_x = 0$.

increases with the increase of the aspect ratio b/a when the inhomogeneity is softer than the matrix, but decreases with the increase of b/a when the inhomogeneity is harder. This figure also shows two limiting cases: the first is concerned with a void ($G^2_L/G^1_L = 0$) and the second with a rigid inhomogeneity ($G^2_L/G^1_L = \infty$).

Finally, Figs 7 and 8 show the strong dependence of the electroelastic field upon the far-field loading. Figure 7 shows contours of constant shear stress ratio $\sigma_{zy}/\sigma^0_{zy}$ due to a remote applied load of $\sigma^0_{zx} = 0$, $\sigma^0_{zy} = 5\times10^7$ N/m^2, $E^0_x = 0$ and $E^0_y = 10^6$ V/m. Figure 8 shows contours of $\sigma_{zy}/\sigma^0_{zy}$ for the case where $\sigma^0_{zx} = 5\times10^7$ N/m^2, $\sigma^0_{zy} = 0$, $E^0_x = 10^6$ V/m and $E^0_y = 0$ for the same material system. From these figures one can observe the difference between contours of the shear stress as a result of the externally applied mechanical and electric loads. Although severe concentrations are observed near the interface, along the minor radius of the inhomogeneity in both cases, the contour shape in these two figures is quite different. For example, σ_{zy} is symmetric about the x- and y-axes as depicted in Fig. 7, while anti-symmetric about the origin as shown in Fig. 8.

5. CONCLUDING REMARKS

A general solution is provided for the elliptical inhomogeneity problem in piezoelectric materials under antiplane shear and inplane electric field. The explicit forms of the electroelastic fields in both the inhomogeneity and the matrix are obtained using the complex variable method. A convenient form of the change of the electric enthalpy due to the presence of an inhomogeneity was also obtained. The electroelastic field concentrations and the change of electric enthalpy were evaluated for different test cases and were found to be strongly dependent upon the material mismatch, the aspect ratio of the inhomogeneity and the remote loading condition. Specifically, the results show that an elastic inhomogeneity can be treated as a rigid body when the shear moduli ratio $G^2_L/G^1_L \geqslant 5$ and a dielectric inhomogeneity can be treated as a conductor when the dielectric moduli ratio $k^2_{11}/k^1_{11} \geqslant 5$. They also reveal that the electric enthalpy increases with increasing aspect

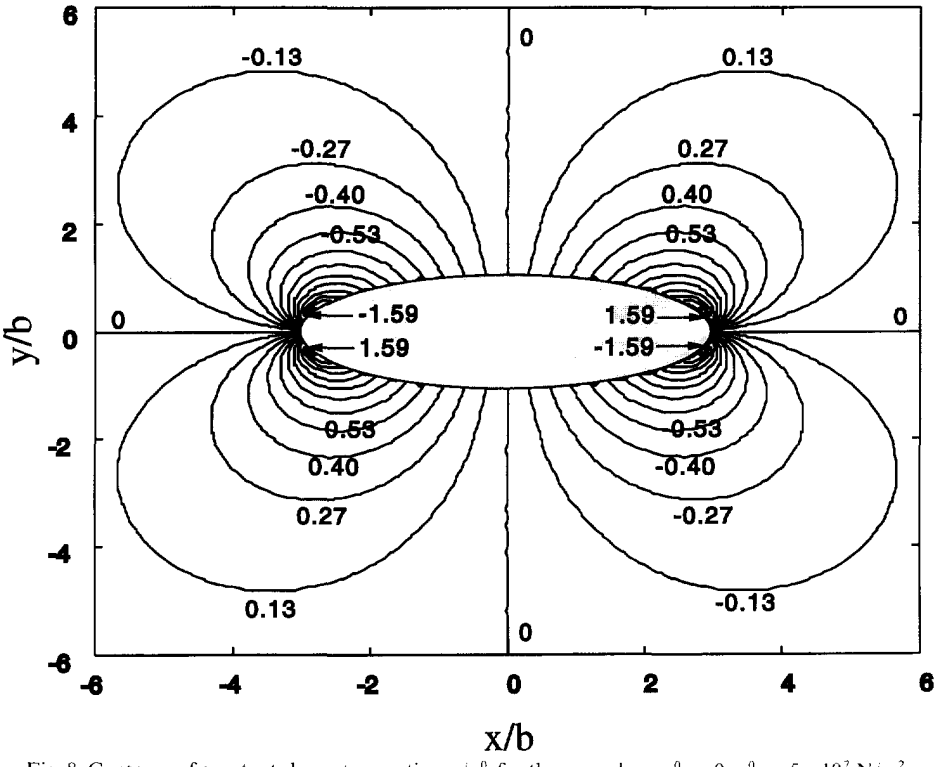

Fig. 8. Contours of constant shear stress ratio $\sigma_{zy}/\sigma_{zy}^0$ for the case where $\sigma_{zy}^0 = 0$, $\sigma_{zx}^0 = 5 \times 10^7$ N/m^2, $E_y^0 = 0$ and $E_x^0 = 10^6$ V/m.

ratio of a relatively softer inhomogeneity ($G_L^2/G_L^1 < 1$) and decreases with a harder inhomogeneity ($G_L^2/G_L^1 > 1$).

Acknowledgements—This work was supported by the Natural Sciences and Engineering Research Council of Canada (NSERC), Ontario Centre for Materials Research (OCMR) and ALCOA Foundation of USA. Partial support of Dr Z. Zhong has also been provided by the National Natural Science Foundation of China.

REFERENCES

Barnett, D. M. and Lothe, J. (1975). Dislocation and line charges in anisotropic piezoelectric insulators. *Physics Statistical Solutions (b)* **67,** 105–111.

Benveniste, Y. (1992). The determination of the elastic and electric fields in a piezoelectric inhomogeneity. *Journal of Applied Physics* **72,** 1082–1095.

Chen, T. (1993). Piezoelectric properties of multiphase fibrous composites: some theoretical results. *Journal of Mechanics of Physical Solids* **41,** 1781–1794.

Deeg, W. F. (1980). The analysis of dislocation, crack and inclusion problems in piezoelectric solids. Ph.D. dissertation, Stanford University.

Dunn, M. and Taya, M. (1993). Micromechanics predictions of the effective electro-elastic moduli of piezoelectric composites. *International Journal of Solids and Structures* **30,** 161–175.

Dunn, M. (1994a). The effect of crack face boundary conditions on the fracture mechanics of piezoelectric solids. *Engineering Fracture Mechanics* **48,** 25–39.

Dunn, M. (1994b). Electroelastic Green's functions for transversely isotropic piezoelectric media and their application to the solution of inclusion and inhomogeneity problems. *International Journal of Engineering Science* **32,** 119–131.

Eshelby, J. D. (1957). The determination of the elastic field of an ellipsoidal inclusion and related problems. *Proceedings of the Royal Society A* **241,** 376–396.

Gong, S. X. and Meguid, S. A. (1992). A general treatment of the elastic field of an elliptical inhomogeneity under antiplane shear. *Journal of Applied Mechanics* **59,** S131–S135.

Gong, S. X. and Meguid, S. A. (1993). On the elastic fields of an elliptical inhomogeneity under plane deformation. *Proceedings of the Royal Society of London A* **443,** 457–471.

Liang, J., Han, J. C., Wang, B. and Du, S. Y. (1995). Electroelastic modelling of anisotropic piezoelectric materials with an elliptic inclusion. *International Journal of Solids and Structures* **32,** 2989–3000.

McMeeking, R. M. (1989) Electrostrictive stresses near crack-like flaws. *Z. Angew. Mathematical Physics* **40,** 615–627.

Pak, Y. E. (1990). Crack extension force in a piezoelectric material. *Journal of Applied Mechanics* **57,** 647–653.

Pak, Y. E. (1992). Circular inclusion problem in antiplane piezoelectricity. *International Journal of Solids and Structures* **29,** 2403–2419.
Schulgasser, K. (1992) Relationships between the effective properties of transversely isotropic piezoelectric composites. *Journal of Mechanics and Physics of Solids* **40,** 473–479.
Sosa, H. A. and Pak, Y. E. (1990) Three-dimensional eigenfunction analysis of a crack in a piezoelectric material. *International Journal of Solids and Structures* **16,** 1–15.
Suo, Z., Kuo, C. M., Barnett, D. M. and Wills, J. R. (1992) Fracture mechanics for piezoelectric ceramics. *Journal of Mechanics and Physics of Solids* **40,** 739–765.
Wang, B. (1992). Three-dimensional analysis of an ellipsoidal inclusion in a piezoelectric material. *International Journal of Solids and Structures* **29,** 293–308.
Yang, W. and Suo, Z. (1994). Cracking in ceramic actuators caused by electrostriction. *Journal of Mechanics and Physics of Solids* **42,** 649–663.

APPENDIX

$$I_0^{(1)} = \lambda_1 + \lambda_3 \tag{A1.1}$$

$$J_0^{(1)} = \lambda_1 + \lambda_3 \tag{A1.2}$$

$$L_0^{(1)} = \lambda_2 + \lambda_4 \tag{A1.3}$$

$$N_0^{(1)} = \lambda_2 + \lambda_4 \tag{A1.4}$$

$$I_0^{(3)} = \lambda_5 + \lambda_7 \tag{A1.5}$$

$$J_0^{(3)} = \lambda_5 + \lambda_7 \tag{A1.6}$$

$$L_0^{(3)} = \lambda_6 + \lambda_8 \tag{A1.7}$$

$$N_0^{(3)} = \lambda_6 + \lambda_8 \tag{A1.8}$$

$$I_0^{(2)} = \frac{1}{\mu_1}\left(\lambda_1 - \lambda_3 + \frac{\lambda_1 + \lambda_3}{R^2}\right) \tag{A1.9}$$

$$J_0^{(2)} = \frac{1}{\mu_1}\left(\lambda_1 + \lambda_3 + \frac{\lambda_1 - \lambda_3}{R^2}\right) - 1 \tag{A1.10}$$

$$L_0^{(2)} = \frac{1}{\mu_1}\left(\lambda_2 - \lambda_4 + \frac{\lambda_2 + \lambda_4}{R^2}\right) \tag{A1.11}$$

$$N_0^{(2)} = \frac{1}{\mu_1}\left(\lambda_2 + \lambda_4 + \frac{\lambda_2 - \lambda_4}{R^2}\right) \tag{A1.12}$$

$$I_0^{(4)} = \frac{1}{\mu_2}\left(\lambda_5 - \lambda_7 + \frac{\lambda_5 + \lambda_7}{R^2}\right) \tag{A1.13}$$

$$J_0^{(4)} = \frac{1}{\mu_2}\left(\lambda_5 + \lambda_7 + \frac{\lambda_5 - \lambda_7}{R^2}\right) \tag{A1.14}$$

$$L_0^{(4)} = \frac{1}{\mu_2}\left(\lambda_6 - \lambda_8 + \frac{\lambda_6 + \lambda_8}{R^2}\right) \tag{A1.15}$$

$$N_0^{(4)} = \frac{1}{\mu_2}\left(\lambda_6 + \lambda_8 + \frac{\lambda_6 - \lambda_8}{R^2}\right) - 1 \tag{A1.16}$$

with

$$\lambda_1 = \frac{1}{\delta_1}\left\{\left[\left(1 + \frac{1}{\mu_2}\right) - \left(1 - \frac{1}{\mu_2}\right)\frac{1}{R^2}\right] + \frac{e_{15}^1}{G_L^1 k_{11}^2}\left[(e_{15}^1 + e_{15}^2) + (e_{15}^1 - e_{15}^2)\frac{1}{R^2}\right]\right\} \tag{A1.17}$$

$$\lambda_2 = \frac{1}{\delta_1}\left\{\frac{e_{15}^1}{k_{11}^1}\left[\left(1 + \frac{1}{\mu_2}\right) - \left(1 - \frac{1}{\mu_2}\right)\frac{1}{R^2}\right] - \frac{1}{k_{11}^2}\left[(e_{15}^1 + e_{15}^2) + (e_{15}^1 - e_{15}^2)\frac{1}{R^2}\right]\right\} \tag{A1.18}$$

$$\lambda_3 = \frac{1}{\delta_2}\left\{\left[\left(1+\frac{1}{\mu_2}\right)+\left(1-\frac{1}{\mu_2}\right)\frac{1}{R^2}\right]+\frac{e_{15}^1}{G_L^1 k_{11}^2}\left[(e_{15}^1+e_{15}^2)-(e_{15}^1-e_{15}^2)\frac{1}{R^2}\right]\right\} \tag{A1.19}$$

$$\lambda_4 = \frac{1}{\delta_2}\left\{\frac{e_{15}^1}{k_{11}^1}\left[\left(1+\frac{1}{\mu_2}\right)+\left(1-\frac{1}{\mu_2}\right)\frac{1}{R^2}\right]-\frac{1}{k_{11}^2}\left[(e_{15}^1+e_{15}^2)-(e_{15}^1-e_{15}^2)\frac{1}{R^2}\right]\right\} \tag{A1.20}$$

$$\lambda_5 = -\frac{1}{\delta_1}\left\{\frac{e_{15}^1}{G_L^1}\left[\left(1+\frac{1}{\mu_1}\right)-\left(1-\frac{1}{\mu_1}\right)\frac{1}{R^2}\right]-\frac{1}{G_L^2}\left[(e_{15}^1+e_{15}^2)+(e_{15}^1-e_{15}^2)\frac{1}{R^2}\right]\right\} \tag{A1.21}$$

$$\lambda_6 = \frac{1}{\delta_1}\left\{\left[\left(1+\frac{1}{\mu_1}\right)-\left(1-\frac{1}{\mu_1}\right)\frac{1}{R^2}\right]+\frac{e_{15}^1}{G_L^2 k_{11}^1}\left[(e_{15}^1+e_{15}^2)+(e_{15}^1-e_{15}^2)\frac{1}{R^2}\right]\right\} \tag{A1.22}$$

$$\lambda_7 = -\frac{1}{\delta_2}\left\{\frac{e_{15}^1}{G_L^1}\left[\left(1+\frac{1}{\mu_1}\right)+\left(1-\frac{1}{\mu_1}\right)\frac{1}{R^2}\right]-\frac{1}{G_L^2}\left[(e_{15}^1+e_{15}^2)-(e_{15}^1-e_{15}^2)\frac{1}{R^2}\right]\right\} \tag{A1.23}$$

$$\lambda_8 = \frac{1}{\delta_2}\left\{\left[\left(1+\frac{1}{\mu_1}\right)+\left(1-\frac{1}{\mu_1}\right)\frac{1}{R^2}\right]+\frac{e_{15}^1}{G_L^2 k_{11}^1}\left[(e_{15}^1+e_{15}^2)-(e_{15}^1-e_{15}^2)\frac{1}{R^2}\right]\right\} \tag{A1.24}$$

$$\delta_1 = \left[\left(1+\frac{1}{\mu_1}\right)-\left(1-\frac{1}{\mu_1}\right)\frac{1}{R^2}\right]\left[\left(1+\frac{1}{\mu_2}\right)-\left(1-\frac{1}{\mu_2}\right)\frac{1}{R^2}\right]+\frac{1}{G_L^2 k_{11}^2}\left[(e_{15}^1+e_{15}^2)-(e_{15}^1-e_{15}^2)\frac{1}{R^2}\right]^2 \tag{A1.25}$$

$$\delta_2 = \left[\left(1+\frac{1}{\mu_1}\right)+\left(1-\frac{1}{\mu_1}\right)\frac{1}{R^2}\right]\left[\left(1+\frac{1}{\mu_2}\right)+\left(1-\frac{1}{\mu_2}\right)\frac{1}{R^2}\right]+\frac{1}{G_L^2 k_{11}^2}\left[(e_{15}^1+e_{15}^2)-(e_{15}^1-e_{15}^2)\frac{1}{R^2}\right]^2. \tag{A1.26}$$